Cite This: J. Phys. Chem. Lett. 2018, 9, 7137–7145

To Be or Not To Be Protonated: cyclo-N₅ in Crystal and Solvent

Wei Chen, *, * Zhiqiang Liu, * Yinghe Zhao, * Xianfeng Yi, * Zhongfang Chen, *, † Diagram Chen, *, † and Anmin Zheng*,[‡](

ABSTRACT: Pentazole (HN₅) and its anion (cyclo-N₅⁻) have been elusive for nearly a century because of the unstable N₅ ring. Recently, Zhang et al. reported the first synthesis and characterization of the pentazolate anion cyclo- N_5^- in $(N_5)_6(H_3O)_3(NH_4)_4Cl$ salt at ambient conditions (Science 2017, 355, 374). However, whether the cyclo-N₅ in (N₅)₆(H₃O)₃(NH₄)₄Cl salt is protonated or not has been debated (Huang ard Yu, Science, 2018, 359, eaao3672; Jiang et al. Science, 2018, 359, aas8953). Herein, we emuly, ed ab initio molecular dynamics (AIMD) simulations, which can well present the dynamic behavior at realistic experimental conditions, to examine the potential proton tec st. te of cyclo-N₅ in both crystal and dimethyl sulfoxide (DMSO) solvent. Our sinus tions revealed that the protonation reaction of $(N_5)_6(H_3O)_3(NH_4)_4Cl \rightarrow (N_5)_5(N_1H)(H_2O)(H_3O)_2(NH_4)_4Cl$ is thermodynamically spontaneous according to $\Delta G < 0$, and be small energy barrier of 12.6



kJ/mol is not enough to prevent the partial proton α' on α' cyclo- N_5 due to the temperature effect; consequently, both deprotonated and protonated cyclo-N₅ exist in the created Ir comparison, the DMSO so very effect can remarkably reduce the difference of proton affinities among cyclo-N₅-, H₂O and NH₃, and the temperature ence can finally break these hydrogen bonds and lead to the deprotonated cyclo- N_5 \sim DM \sim Solvent. Our AIMD sime then reconcile the recent controversy.

igcup entazole (HN₅) and its anion (*cyclo*-N₅) are the potential constituents of energetic material can be applied in both military and civilian contexts. 1-5 In January 2017, Zhang et al.6 reported the first synthesis and characterization of the pentazolate anion, cyclo- N_5^- , in $(N_5)_6(H_3O)_3(NH_4)_4Cl$ salt at ambient conditions and concluded that cyclo-N5 is stabilized by hydrogen bonding from adjacent H₃O⁺ and NH₄ counterions. Encouraged by this exciting experimental ment, various complexes and salts containing cyclo N - nave been developed as new high-energy-density materials. cyclo- N_5^- can interact with metal ions $(Mn^{2+}, Co^{2^2}, Fc^{2+}, Mg^{2+}, Ag^+, Na^+, Zn^{2+}, Li^+, and <math>Rb^+)^{1-5,7-12}$ to form the all complexes, coordination polymers, and metal-organic frameworks; it can also be stabilized by nanocages (Na) and Na₂₄N₆₀), and Na₂₄N₆₀), and Na₂₄N₆₀), and Na₂₄N₆₀), so manotubes (CNT), and organic ions. Moreover, new materials such as metal pentaz in rameworks have been theoretically predicted. It is not vorthy that very recently Yu et al. investigated the stabilities and possible formation pathways of the pentazo'ate anion at the B3LYP/6-311+ +G** and CCSD(7)/\SbS levels. 17 These results have been illuminating the varhs of theoretical and experimental studies on pentazolit.

However, the precise characterization of cyclo-N₅ is difficult because of the explosive hazard of the (N₅)₆(H₃O)₃(NH₄)₄Cl crystal as the energetic material and the inability of experimental analysis to confirm the position of hydrogen atoms. Modern quantum chemical computations offer an

alternative and also are powerful tools to investigate the structure, and properties of materials. In this regard, in March 2010 Huang and Xu18 challenged Zhang's structural characterhat on. Their density functional theory (DFT) computations and wave functional analysis based on static cluster models in the gas phase suggested that the cyclo-N₅ anion does not exist in the synthesized crystal; instead, its neutral protonated HN5 would be favored over the anion in the reported pentazolate salt via proton transfer. In response, Jiang et al., 19 the research team receiving the comment, insisted on the existence of cyclo-N₅⁻, arguing that Huang et al. 18 used an improper method to access the proton transfer in a solid crystal structure, because the result in the gas phase cannot explain the phenomenon in crystal. Moreover, Jiang et al. 19 also performed the static periodic DFT calculations and liquid NMR spectroscopy to confirm the existence of cyclo-N₅⁻ in the crystal structure. Note that external conditions, especially temperature, could greatly influence the proton transformation in the solid, and the liquid NMR spectrum might not well explain the situation in the crystal structure. Nevertheless, the effects of temperature and solvents have not been considered by Jiang et al. 19 in the above debate. To date, the controversy has not been reconciled, and

Received: September 14, 2018 Accepted: November 5, 2018 Published: November 5, 2018

7137

[‡]State Key Laboratory of Magnetic Resonance and Atomic and Molecular Physics, National Center for Magnetic Resonance in Wuhan, Wuhan Institute of Physics and Mathematics, Chinese Academy of Sciences, Wuhan 430071, P.R. China

Department of Chemistry, University of Puerto Rico, Rio Piedras Campus, San Juan, Puerto Rico 00931, United States [§]University of Chinese Academy of Sciences, Beijing 100049, P.R. China

Supporting Information

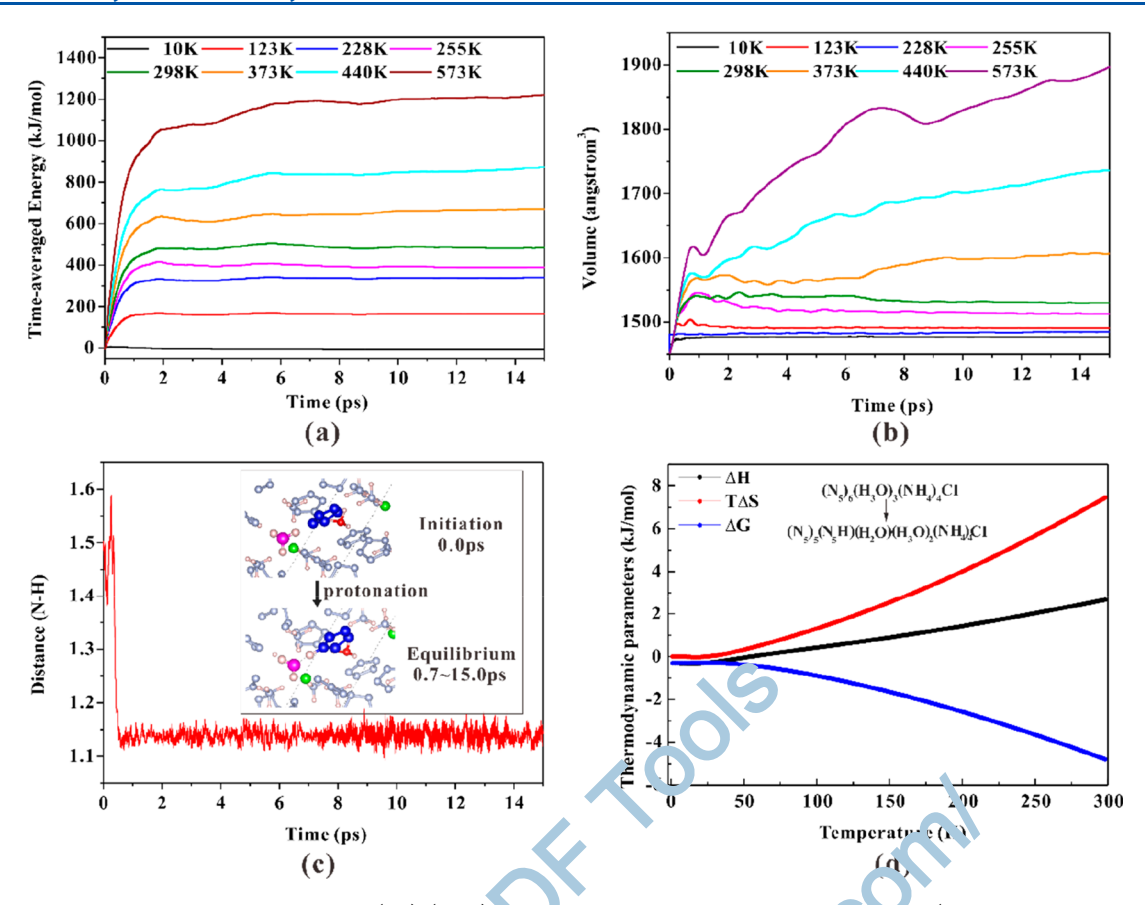


Figure 1. AIMD simulations of NPT ensemble on $(N_5)_6(H_2C)$ (. IH)4Cl crystal under different ter per tures (10, 123, 228, 255, 298, 373, 440, and 573 K) and 1 bar. (a) Time-averaged energy curve, (b, vr.ume curve with timeline, (c) the protection process from $N_5^- \cdots H_3O^+$ to $N_3H \cdots H_2O$ at 123 K, and (d) thermodynamic parameters of $(N_5)_6(H_3O)_3(NH_4)_4Cl \rightarrow (N_5)_5(N_2H_3O)_2(NH_4)_4Cl$ based on static periodic DFT calculations.

the question of whether the cyclo- N_5^- in the possible structure and DMSO solvent is protonated is star or n

Ab initio molecular dynamics (m AMJ) is a powerful computational technique that can better reflect dynamic behaviors at realistic experimental conditions as compared with static DFT calculations. We performed comprehensive AIMD simulation, which can account for temperature and solvent efficient to explore the form of $cyclo-N_5^-$ in $(N_5)_6(H_3O)_3(NH_4)_4$ (1 c. extal and DMSO solvent.

Protonated State of cyclo-N₅⁻ in Crystal. In the rystal, the initial structures and cell parameters were as commized. Our optimized cell parameters are in good agreement with the experimental data (Table S1). The same as reported by Jiang et al., 19 we also found that the cyclo is not spontaneously protonated by H₃O⁺ and NH₄, by static periodic DFT calculation. Starting from the optimized initial structure, the system was simulated in the NOT ensemble at a pressure of 1 bar and eight important experiment temperatures, namely, 10 K (ultralow temperature), 123 K (XRD temperature), 228 K (reaction temperature), 373 K (first decomposition temperature), 440 K (see and decomposition temperature), and 573 K (final decomposition temperature), for 15 ps.

When the temperature is below 298 K, as indicated by the averaged energy and volume fluctuations (Figure 1a,b), the $(N_5)_6(H_3O)_3(NH_4)_4Cl$ system can rapidly reach an equilibrium state. The MD trajectories at 123 K (XRD temperature)

revealed that two cyclo- N_5^- have been protonated to HN_5 at the b.g. using of the simulations, as illustrated in Movie 1. In other words, the protonation of $cyclo-N_5^-$ in $(N_c)_6(H_3O)_3(NH_4)_4Cl$ at 123 K is spontaneous (Figure 1b), which is qualitatively in agreement with Huang's conclusion obtained by using a static gas-phase cluster model 17 and indicates that the extensive hydrogen-bonding interactions between the cations and anions in the crystal 19 are not sufficient to retain all hydrogen atoms in H_3O^+ (see the detailed trajectory in the Supporting Information).

When the temperature reaches 298 K, the temperature effect on the proton-transfer process becomes significant: continuous proton transformation between one H₃O⁺ and three cyclo-N₅⁻ can be observed (see Figure S1 and Movie 2), and the volume change of the $(N_5)_6(H_3O)_3(NH_4)_4Cl$ crystal is within 5.5% (Figure 1b). Further increasing the temperature resulted in the collapse of $(N_5)_6(H_3O)_3(NH_4)_4Cl$ crystal with over 10.7% volume expansion, in agreement with experimental observations. Note that the HN5 can be observed at all these temperatures (see Figure S2). Note that the quantum effect and long-range correlation could influence the proton motion. To consider these effects, we performed ab initio path integral molecular dynamics (AI-PIMD) calculations at 10 K and also performed AIMD simulations using a larger simulation box (i.e., $2 \times 1 \times 1$, $1 \times 2 \times 1$, and $1 \times 1 \times 2$) at 123 K. However, our computations showed that including these factors does not have a significant effect, and our original conclusion holds true (see Figures S3 and S4, and Movie 3).

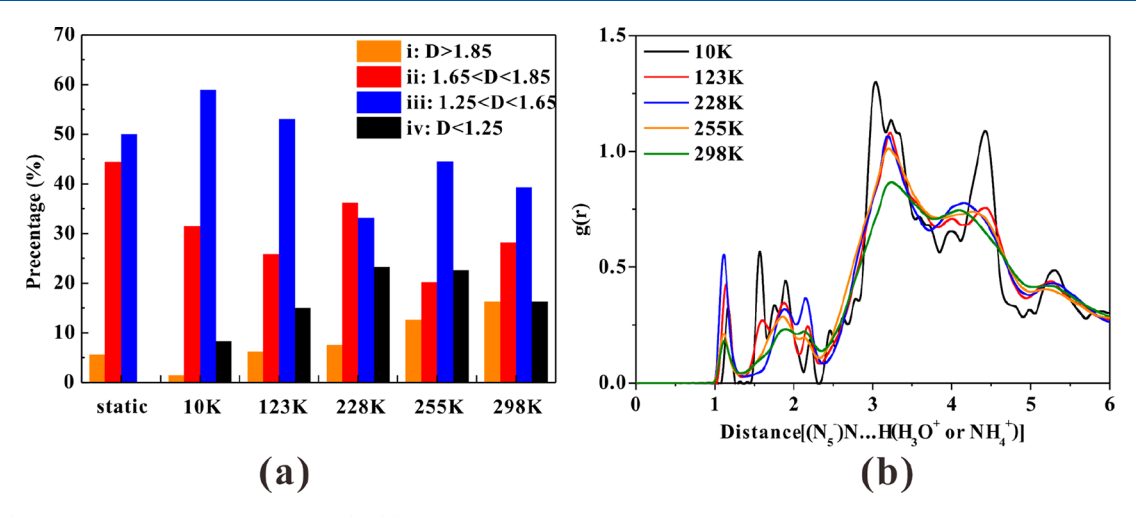


Figure 2. (a) N—H distance distributions and (b) g(r) between hydrogen atoms and the nitrogen atoms of cyclo-N₅⁻ by AIMD simulations under NVE ensemble in the $(N_5)_6(H_3O)_3(NH_4)_4Cl$ crystal at different temperatures.

To investigate the temperature effect, we carried out the thermodynamic analysis of the proton-transfer process, i.e., $(N_5)_6(H_3O)_3(NH_4)_4C1 \rightarrow (N_5)_5(N_5H)(H_2O)_5$ (H₃O)₂(NH₄)₄Cl (Figure 1d). The instantaneous proton transfer to N₅ found in MD simulations can be fully understood from both the negative Gibbs free-energy change $(\Delta G, \Delta G = \Delta H - T\Delta S)$ of this process and the very low energy barrier of 12.6 kJ/mol obtained by static computations. Notably, the ΔG value becomes more negative with increasing temperature because of the positive ΔS value. Thus, from the thermodynamic viewpoint, it is a spontaneous reaction that the proton transfers from H_3O^+ to cyclo- N_5^- to form p of zole. The thermodynamically spontaneous process and the small energy barrier (12.6 kJ/mol) for the protonat on reaction, $(N_5)_6(H_3O)_3(NH_4)_4C1 \rightarrow (N_5)_5(N_5H_7)(H_2O)_5$ (H₃O)₂(NH₄)₄Cl, allow the transformatio 1 b tween N₅ and HN₅ in the crystalline environment even under very low temperature (e.g., 10 K).

Our AIMD simulations at the *NPT* ensemble revealed the existence of HN_5 in the crystal. To certify the presence of HN_5 and examine the behavior and stability of HN_5 under 298 K we further performed 30 ps AIMD simulations under *NVT* ensemble at the temperatures of 10, 123, 228, 255, and 25 % to equilibrate the crystal.

To examine the state of N₅⁻ and hydrogen bong in H₃O⁺··· N_5^- , we employed the atom in molecule (ATM) method²³ to analyze the interaction between N and U u ing Multiwfn software.24 The interaction between N and H ... n be divided to four categories^{25,26} (for detailed classi²c tion, see Table S2). As displayed in Figure 2a, the static less ts (0 K) revealed that the (N_5^-) N···H (H_3O^+) is main very gorized as ii and iii, e.g., the weak and medium hydro, v. bonds, and protonated HN5 does not exist, which is in a rement with Jiang et al.'s periodic DFT computations. 19 With increasing temperature from 10 to 298 K, the cyclo-N procies (HN₅) begins to emerge: the percentage of covile. N-H bond (iv) increases to 15.0% at 123 K, reaches a paxium value of 23.2% at 228 K, up to 22.6% at 255 K, and then declines to 16.3% at 298 K. Such increasing precentage of covalent N-H bond from 10 to 255 K can be explained by the more negative ΔG with the rising of temperature in Figure 1d, because the more negative ΔG will lead to the higher transformed tendency from N5- to HN5 in the crystal.

To get a full picture of the protonation of $cyclo-N_5^-$, we plotted the radial distribution function g(r) between nitrogen atoms of $cyclo-N_5^-$ and all the hydrogen atoms (Figure 2b), which helt visualize the distribution of N–H distances. In general distinct g(r) peaks corresponding to the covalent N–H binc (iv: 0.95–1.25 Å) in HN₅ appear at all temperatures (Figure 2b), indicating that the protonated HN₅ is a permanent and ineradicable species under the temperatures we studied. Note that the $(N_5)_c(H_3O)_3(NH_4)_4Cl$ salt is very similar to the substance in the lithium imide/amide systems; the possible existence of crenkel defects could affect the protonated states of $c_c clo-N_5^-$ in the crystal because the Frenkel defect is $C_c clo-N_5^-$ in the crystal because the Frenkel defect is $C_c clo-N_5^-$ and $C_c clo-N_5^-$.

Protonate State of cyclo- N_5^- in Dimethyl Sulfoxide (DMSO) Solvent. Our AIMD simulations strongly confirmed the dominance of N_5^- and the existence of HN_5 in the $(N_5, (H_3O)_3(NH_4)_4Cl$ crystal under experimental conditions. Then, how about the situation in a solvent?

To address this question, we performed molecular dynamics simulations with explicit solvent models. In our model, there are 30 DMSO solvent molecules in a $15 \times 15 \times 15$ cubic box. The $HN_5_H_2O$, $N_5^-_H_3O^+$, and $N_5^-_NH_4^{+}$ complexes, whose existence was revealed by our AIMD simulations in the crystal, were put separately into the solvent system. Note that DMSO solvent can easily dissolve the $(N_5)_6(H_3O)_3(NH_4)_4Cl$ crystal, as indicated by the very narrow ¹⁵N NMR. ⁶ Moreover, the N₅/ H₃O⁺/NH₄⁺ fragments and DMSO solvent can form good hydrogen-bonding networks (Figure S6). Therefore, the rest of the components in the crystal can be approximately ignored in the theoretical calculations because of their insignificance and the limitation of the current computational resources. The initial structures were first simulated by 1 ns MD simulation in the NVT ensemble at 298 K based on the Dreiding force field, 28 i.e., MM/MD, and further optimized and dynamically simulated at the PBE-D3/DZVP level of theory.

According to our MM/MD simulations, the strong electrostatic interaction between charged species drives H_3O^+ or NH_4^+ surrounding the $cyclo\cdot N_5^-$ in $N_5^-_H_3O^+$ and $N_5^-_NH_4^+$ systems, while in the $HN_5_H_2O$ system, the neutral H_2O and HN_5 interact by $(H_2O)O\cdots H(HN_5)$ hydrogen bonding. Note that the $N_5^-_H_3O^+$ complex can adopt two different configurations: In the first configuration, denoted as

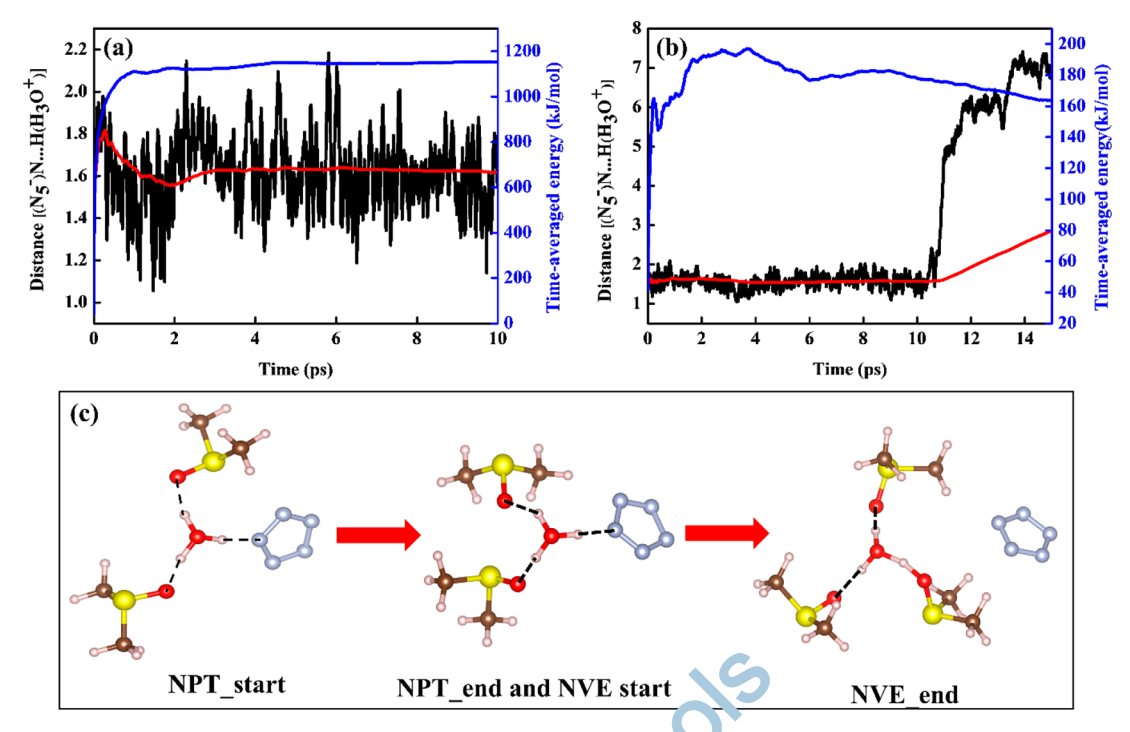


Figure 3. Time-averaged energy (blue) and $[(N_5^-)N\cdots H(H_3O^+)]$ distances (blac'...) suntaneous values, red: time-averaged values) of $N_5^-H_3O^+$ complexes in (a) NPT and (b) subsequent NVE ensembles with 30 DMSO olecyle by AIMD simulations, (c) napshots of configurations at the start and end of simulations in NPT and NVE ensembles, the black dashed lines are hydrogen bonds. (other DMSO molecules are not shown for clarity).

 $N_5^-H_3O^+$, H_3O^+ interacts with *cyclo-* N_5^- by hydrogen bonding. In the second configuration, denoted as $N_5^-N_5^+$ H_3O^+ is tightly captured by three DMSO molecules via $(H_3O^+)H\cdots O(DMSO)$ hydrogen bond interactions; consequently, the *cyclo-* N_5^- could interact only with the Coatom of H_3O^+ , rather than Hoatoms. Thus, four system containing these complexes, namely, $N_5^-H_3O^+$, $N_5^-OF_3^-$, $N_5^-H_3O^+$, and $N_5^-NH_4^+$ (detailed structures of these four initial structures are provided in Figure S6) were subsequently investigated by the precise AIMD simulations in the *NPT* ensemble.

The system initially containing the N₅-H₃O⁺ complex car quickly reach equilibrium at 298 K (Figure 3a), and the curv of $(N_5^-)N\cdots H(H_3O^+)$ distance reveals that the interactions we mostly strong hydrogen bonding, with only a few N-H covalent bonding (with N-H distances <1.25 Å). However, the stability of this hydrogen bond-containing s, ste n is rather low, as revealed by our subsequent 15 p. VE simulations. This hydrogen bond can remain stable for only ~10 ps and finally breaks with obvious energy rease (Figure 3b), leaving one hydrogen of H₃O⁺ taken away by DMSO (Figure 3c; see Movie 4 for details). Sir, il, r1, for the system initially containing the N_5^- O H_3^+ co. 9ex, the cyclo- N_5^- cannot take hydrogen away from the H.O. which is hydrogen bonded with DMSO, as seen from the mapshots in Figure 4 and the over 6 Å N-O distance in Figure S4. Thus, because of the strong ability of DMSO Scarture H₃O+, the chance for cyclo-N₅- to interact with H_3O^+ to form either $N_5^- H_3O^+$ or $N_5^- OH_3^+$ complexes is rather slim.

Can the HN_5 originally existing in the $(N_5)_6(H_3O)_3(NH_4)_4Cl$ crystal preserve its protonated form in DMSO solution? Our AIMD simulations on the $HN_5_H_2O$ system in the *NPT* ensemble revealed that the covalent N-H bond quickly breaks; the lost H first forms a hydrogen bond

 $[(N_5^-)N\cdots H(H_3O^+)]$ with H_3O^+ ; finally this hydrogen bond is broken by the effect of temperature, and $cyclo-N_5^-$ departs from H_3O^+ similar to what occurs in $N_5^-H_3O^+$ and $N_5^-OH_3^+$ systems. Figure 4).

We also can med the possibility for the $N_5^-NH_4^+$ complex. No \circ that Jiang et al. Pointed out that the NH3 molecule as a stronger proton affinity than H2O, indicating the in the difficulty for $cyclo-N_5^-$ to be protonated by NH4⁺. This expectation was confirmed by AIMD simulations: the N_5^- and NH4⁺ units separate from each other along the simulations Figures 4 and S5).

Our AIMD simulations showed that $cyclo-N_5^-$ can be protonated in the crystal, but it preserves the free anion form in the DMSO solvent; in other words, there is $cyclo-N_5^-$ of $(N_5)_6(H_3O)_3(NH_4)_4Cl$ in DMSO solution (Table 1). Why can the $cyclo-N_5^-$ not be protonated by H_3O^+ or NH_4^+ in the DMSO environment? To gain further insights into the different behavior in the crystal and solvent, we calculated the proton affinities (PAs) in both the gas phase and DMSO solvent (Table 2; see Supporting Information for details).

Our used theoretical levels (M06-2X-D3 and PBE-D3) can reproduce the experimental PA values for NH₃, H₂O, and DMSO in the gas phase (the error between experiment and calculation is less than 9 kJ/mol) and are expected to well predict PA values of other related systems in this work. *cyclo*-N₅⁻ (PA = 1332.8 kJ/mol) has a much higher PA than H₂O (691.9 kJ/mol) and NH₃ (845.0 kJ/mol at M06-2X-D3 level of theory), which can explain qualitatively the protonated HN₅ in the isolated gas-phase H₃O⁺_N₅⁻ complex model reported by Huang et al. ¹⁸ and the appearance of HN₅ in (N₅)₆(H₃O)₃(NH₄)₄Cl crystal revealed by our AIMD simulations. Note that proton affinity is a reliable parameter to determine the basicity of a neutral atom or molecule or an anion in the free state. However, the PA computations can

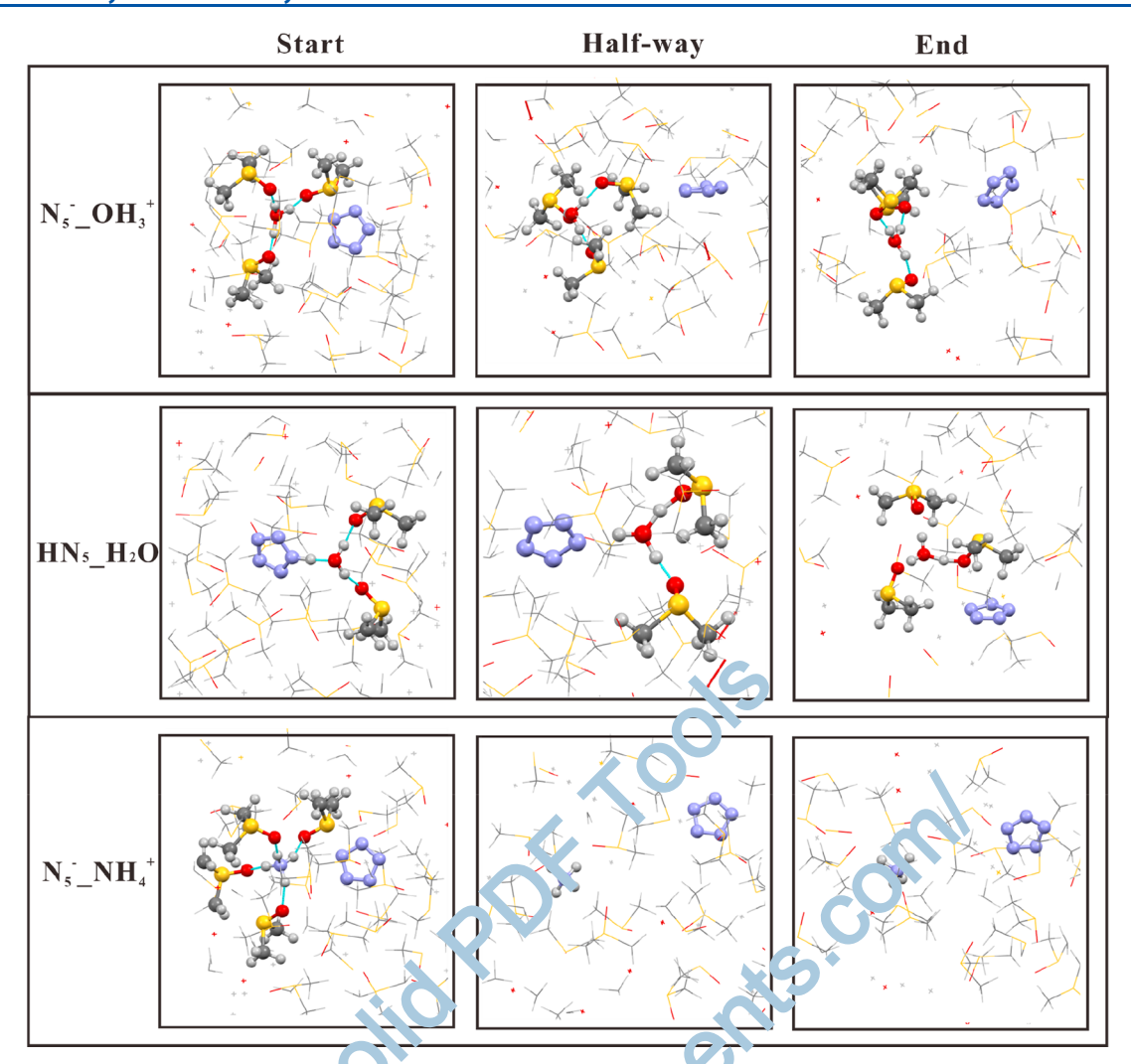


Figure 4. Snapshots of $N_5^-OH_3^+$, $HN_5_F_2O_{21}^-N_5^-NH_4^+$ systems in NPT engine at 298 K. The hydrogen bonds are denoted by cyan lines.

Table 1. Summary of Protonated State in Different Systems in DMSO Solvent after AIMD Simulations at 298 K in NPT and the Subsequent NVE Ensembles

system	Iinitial interaction ^a	NPT^b), v/F ,,
N ₅ _H ₃ O ⁺	H-bonding	a few protonations, mostly H bonding	p. ytonation
N ₅ ⁻ _OH ₃ ⁺	van der Waals interaction	no protonation	o protonation
HN ₅ _H ₂ O	covalent bond	a few protonations, mostly H boading	no protonation
$N_5^-NH_4^+$	van der Waals interaction	no protopati n.	no protonation

^aThe initial interaction between ni^a. On of cyclo-N₅⁻ and hydrogen of H₃O⁺ or NH₄⁺. ^bThe protonage state of cyclo-N₅⁻.

provide only a qualit α e order for the relative basicity of H_2O , NH_3 , and N_5^- by an official give a quantitative result because the charge of N_7 and N_5 hy and N_5 hy

recause the PA values in the gas phase might differ significantly from those in the liquid phase because of the solvent effect, we computed their PA values in the solvent using both the implicit SMD solvation model and the explicit model.²⁹ This implicit model can increase the PA values of NH₃, H₂O, and DMSO (by ca. 230-370 kJ/mol), while it decreases the PA value of cyclo-N₅ by ca. 210 kJ/mol, consequently reducing the PA difference between H2O and cyclo-N₅ from ca. 640 kJ/mol in the gas phase to ca. 64 kJ/ mol in the solvent at the M06-2X-D3 level of theory (Table 2). To deeply investigate the influence of the realistic hydrogenbonding interactions between the solvent (DMSO) and solutes (NH₃, NH₄⁺, H₂O, and H₃O⁺), ³⁰ besides the empirical implicit solvation model, we also calculated the PA values of H₂O and NH_3 combined with different numbers (n = 1-3) of DMSO solvent molecules to approach the explicit solvent model as much as possible. As the number of DMSO molecules increase, the PA values of both H₂O and NH₃ increase, confirming that the DMSO solvent can increase the PA of H₂O and NH₃, as found in the implicit solvent model. Thus, the solvent effect of DMSO is responsible for the greatly reduced PA differences among cyclo-N₅-, H₂O, NH₃, and DMSO species.

More specifically, for the $N_5^-H_3O^+$ complex, the minimum on the potential energy surface (PES) along the $(N_5^-)N\cdots$ $H(H_3O^+)$ distance in the gas phase significantly differs from

Table 2. Proton Affinity (kJ/mol) of cyclo-N₅⁻, H₂O, NH₃, and DMSO Calculated in the Gas Phase and in the Solvent Using Implicit SMD and Explicit Solvent Models^a

	gas phase		implicit solvent	number of DMSO in explicit $model^c$		
species	exptl ^b	calc ^c	calc ^c	1	2	3
cyclo-N ₅		1332.8/1351.1	1124.3/1140.6			
H_2O	691.0	691.9/ 696.9	1060.0/ 1068.2	947.3/ 946.3	1014.2/ 1021.2	
NH_3	853.6	845.0/854.1	1175.3/1185.1	992.4/ 999.2	1049.0/1063.3	1083.4/ 1090.1
DMSO	884.4	886.6/880.4	1109.9/1110.1			

^aThe number of DMSO molecules in the explicit model (n = 1-3) of DMSO is also given. ^bExperimental values reported by Hunter et al. ³¹ ^cCalculated values at the M06-2X-D3 (in roman type) and PBE-D3 (in bold) levels of theory.

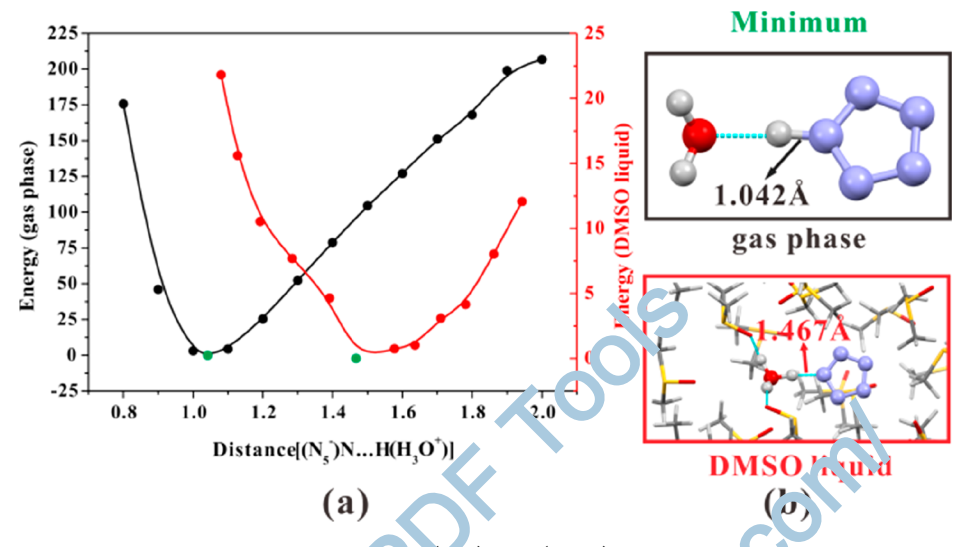


Figure 5. (a) Potential energy surface curve along the direction of $(N_5^-)N\cdots H(H_3O^+)$ distance in the $N^-H_3O^+$ system in the gas phase (black) and DMSO liquid (red); (b) minimum energy structures (h, drogen bonds are denoted by dated lines) (unit: kJ/mol).

In summary, to understand and post tially reconcile the recent controversy about the proton ten state of $cyclo-N_5^-$, we performed AIMD simulations by the can better model the realistic conditions of $(N_5)_6(H_5)_3(NH_4)_4Cl$ in the crystalline environment and DMSO solvent. The presence of the $cyclo-N_5^-$ differs significantly in the crystal and liquid states. In $(N_5)_6(H_3O)_3(NH_4)$ concretely the crystal and liquid states. In the temperature effect, the dominant unproton transfer and the temperature effect, the dominant unprotonated $cyclo-N_5^-$ coexists with its protonated N_5H even at the super low temperature of 10 K; the protonated HN_5 has 15% at 123 K and can reach a maximum percentage of 23.2% at 228 K. In contrast, in the DMSO solvent, the solvent effect significantly narrows the proton affinity difference between $cyclo-N_5^-$ and H_2O (or NH_3), and the temperature effect

further driv's 'he existence of only unprotonated *cyclo-N₅*", which w's in mbiguously identified by the single ¹⁵N peak in the liqu'ic. N'MR experiment. Our AIMD simulations not only rec'nc'le the recent controversy but also call for more at vinion to considering external conditions, such as temperative and solvent, for structural elucidations and property rudies in both experimental and theoretical investigations.

■ COMPUTATIONAL METHODS

CP2K software³² was employed to explore the dynamic behavior of $(N_5)_6(H_3O)_3(NH_4)_4Cl$ in solid and liquid states. All the density functional theory computations were carried out using the PBE-D3 method. ^{33,34} For $(N_5)_6(H_3O)_3(NH_4)_4Cl$ in the solid state, the triple- ζ valence plus polarization (TZVP) basis set³⁵ and the Goedecker—Teter—Hutter (GTH) pseudopotentials^{36,37} were used, while the smaller basis set, namely, double- ζ valence plus polarization (DZVP),³⁵ was used for the much larger liquid systems, which contain 30 DMSO molecules and four complexes $(N_5^-H_3O^+,N_5^-OH_3^+,HN_5_H_2O,$ and $N_5^-NH_4^+)$ within a $15 \times 15 \times 15$ cubic box. During the SCF procedure, a 360 Ry density CUTOFF criterion with the finest grid level was employed, together with multigrids number 4 (NGRID 4 and REL CUTOFF 70).

The time steps in liquid and solid states were both set to 1 fs. In the solid, $(N_5)_6(H_3O)_3(NH_4)_4Cl$ was simulated in the 15 ps *NPT* ensemble (*constant temperature and pressure using a flexible cell*) at temperatures of 10, 123, 228, 255, 298, 373, 440, and 573 K, which rely on a canonical sampling through

velocity rescaling (CSVR) thermostat³⁸ with a time constant of 100 fs to ensure fast thermal equilibration; afterward, 30 ps MD simulations of the *NVE* ensemble at several temperatures (10, 123, 228, 255, and 298 K) were used to count the percentage of HN₅. The quantum effects could influence the proton motion, especially at ultralow temperature, and the ab inito path integral molecular dynamics (AI-PIMD) was employed to consider the quantum effects at 10 K. In liquid systems, $N_5^- H_3 O^+$, $N_5^- O H_3^+$, $H N_5 H_2 O$, and $N_5^- N H_4^+$ complexes in DMSO environment were performed starting with a 10 ps equilibration run to initialize the systems, followed by the production run of 15 ps to obtain a sufficient sampling of the phase space.

To obtain the energy barrier of the proton transfer in the solid, i.e., the process of $(N_5)_6(H_3O)_3(NH_4)_4Cl\rightarrow (N_5)_5(N_5H)(H_2O)(H_3O)_2(NH_4)_4Cl$, the transition state was optimized by the Dimer method. On the basis of the optimized structures and frequencies of $(N_5)_6(H_3O)_3(NH_4)_4Cl$ and $(N_5)_5(N_5H)(H_2O)_4(H_3O)_2(NH_4)_4Cl$, the thermodynamic analysis of this process was carried out by TAMkin software.

The proton affinity calculations were performed at the PBE^{33} and $M06\text{-}2X^{41}$ level of theory with consideration of Grimme's dispersion correction $(DFT\text{-}D3)^{34}$ using Dunning basis sets cc-PVTZ. 42,43 The PA values in the gas phase were directly calculated according to the equation

$$PA(gas) = E(X) - E(HX^{+})$$

$$(X = N_{s}^{-}, H_{2}O, NH_{3}, and DMSO)$$

In liquid, the implicit solvent model, SMD,⁴⁴ was us d of describe the species, and the corresponding PA valuative were calculated following the equation

$$PA(liquid) = E(X_SMD) - E(HX^+_SMD)$$

$$(X = N_5^-, H_2O, NH_3, and DMSO)$$

where $E(X_SMD)$ and $E(HX^+_SMD)$ are the total energies of X and HX^+ in the SMD solvent model, respectively.

Moreover, different numbers of DMSO molecules combined with $\rm H_2O$ and $\rm NH_3$ were used to realize the explicit solvent model as much as possible, and the PA equation can be verifted

PA(liquid) =
$$E(X_nDMSO) - E(HX_nDMSO)$$

(X = H₂O and NH₃; $n = 1-3$)

where $E(X_nDMSO)$ and $E(HX^+_nDMSO)$ are the total energies of X and HX^+ , respectively, c., bined with different numbers (n) of DMSO molecules. An chese PA calculations were performed using *Gaussian* \mathbb{C}^Q (version B.01).⁴⁵

Similar to the PA calculations the potential energy surface (PES) was scanned along the direction of N–H bond in $N_5^-H_3O^+$ and $N_5^-NH_4^+$ complexes under three conditions, i.e., gas phase, implies colvent model (SMD), and explicit solvent model. The two conditions can be easily carried out by Gaussian 09, and the explicit solvent model was represented by 30 DMSO molecules in a 15 × 15 × 15 box via VASP code. To realize the PES scan in the explicit solvent model, $N_5^-H_3O^+$ and $N_5^-NH_4^+$ complexes were first optimized to minima without any constraints in DMSO solution. Subsequently, a series of structures with N–H distance ranging from 0.8 to 2.0 Å were optimized. During the

optimization, the N-H distance was fixed by freezing N and H atoms, but other atoms were relaxed.

ASSOCIATED CONTENT

S Supporting Information

The Supporting Information is available free of charge on the ACS Publications website at DOI: 10.1021/acs.jp-clett.8b02841.

Additional calculation details and results (PDF)

Movie 1: Trajectory for the proton transfer between H_3O^+ and $cyclo-N_5^-$ in the $(N_5)_6(H_3O)_3(NH_4)_4Cl$ crystal at 123 K (XRD temperature) and 1 bar (MPG)

Movie 2: Trajectory for the proton transfer between H_3O^+ and $cyclo-N_5^-$ in the $(N_5)_6(H_3O)_3(NH_4)_4Cl$ crystal at 298 K (room temperature) and 1 bar (MPG)

Movie 3: Trajectory for the proton transfer between H_3O^+ and $cyclo-N_5^-$ in the $(N_5)_6(H_3O)_3(NH_4)_4Cl$ crystal at 10 K (super low temperature) and 1 bar (MPG)

Movie 4: Trajectory for the HN₅_H₂O complex in DM 5 solvent at 298 K (room temperature) and 1 bar

THOR INFORMATION

Corresponding Authors

*E-mail: zhenganm@wipm.a cn. *E-mail: zhongfangchen()gn ail.com.

ORCID (

Zhiqiang Liu: 0° ω-00°3-2872-0125 Yinghe Zhao: 00° J002-2331-8973 Zhongfang Ch`n: 0000-0002-1445-9184 Anmin Theng: 0000-0001-7115-6510

Not

The authors declare no competing financial interest.

ACKNOWLEDGMENTS

This work was supported in China by the National Natural Science Foundation of China (Nos. 21522310, 21473244, and 91645112), and Natural Science Foundation of Hubei Province of China (2018CFA009), and Key Research Program of Frontier Sciences, CAS (No. QYZDB-SSW-SLH026) and in the United States by the National Science Foundation-Centers of Research Excellence in Science and Technology (NSF-CREST Center) for Innovation, Research and Education in Environmental Nanotechnology (CIRE2N) (Grant No. HRD-1736093) and by NASA (Grant No. 80NSSC17M0047).

REFERENCES

- (1) Xu, Y. G.; Wang, Q.; Shen, C.; Lin, Q. H.; Wang, P. C.; Lu, M. a. Series of Energetic Metal Pentazolate Hydrates. *Nature* **2017**, *549*, 78–81.
- (2) Christe, K. O. Polynitrogen Chemistry Enters the Ring. *Science* **2017**, 355, 351–351.
- (3) Sun, C. G.; Zhang, C.; Jiang, C.; Yang, C.; Du, Y.; Zhao, Y.; Hu, B. C.; Zheng, Z. S.; Christe, K. O. Synthesis of AgN_5 and Its Extended 3D Energetic Framework. *Nat. Commun.* **2018**, *9*, 1269.
- (4) Laniel, D.; Weck, G.; Gaiffe, G.; Garbarino, G.; Loubeyre, P. High-Pressure Synthesized Lithium Pentazolate Compound Metastable under Ambient Conditions. *J. Phys. Chem. Lett.* **2018**, *9*, 1600–1604.

- (5) Arhangelskis, M.; Katsenis, A. D.; Morris, A. J.; Friscic, T. Computational Evaluation of Metal Pentazolate Frameworks: Inorganic Analogues of Azolate Metal-Organic Frameworks. *Chem. Sci.* **2018**, *9*, 3367–3375.
- (6) Zhang, C.; Sun, C. G.; Hu, B. C.; Yu, C. M.; Lu, M. Synthesis and Characterization of the Pentazolate Anion Cyclo- N_5^- in $(N_5)_6(H_3O)_3(NH_4)_4$ Cl. Science **2017**, 355, 374–376.
- (7) Xu, Y.; Wang, P.; Lin, Q.; Lu, M. A Carbon-Free Inorganic-Metal Complex Consisting of an All-Nitrogen Pentazole Anion, a Zn (ii) Cation and H₂O. *Dalton. Trans.* **2017**, *46*, 14088–14093.
- (8) Zhang, C.; Yang, C.; Hu, B.; Yu, C.; Zheng, Z.; Sun, C. A Symmetric $Co(N_5)_2(H_2O)_4$ ·4 H_2O High-Nitrogen Compound Formed by Cobalt(II) Cation Trapping of a Cyclo- N_5 ⁻ Anion. Angew. Chem., Int. Ed. **2017**, 56, 4512–4514.
- (9) Williams, A. S.; Steele, B. A.; Oleynik, I. I. Novel Rubidium Poly-Nitrogen Materials at High Pressure. *J. Chem. Phys.* **2017**, *147*, 234701.
- (10) Laniel, D.; Weck, G.; Gaiffe, G.; Garbarino, G.; Loubeyre, P. High-Pressure Synthesized Lithium Pentazolate Compound Metastable under Ambient Conditions. *J. Phys. Chem. Lett.* **2018**, *9*, 1600–1604.
- (11) Xu, Y.; Wang, P.; Lin, Q.; Mei, X.; Lu, M. Self-Assembled Energetic 3D Metal-Organic Framework $[Na_8(N_5)_8(H_2O)_3]_n$ Based on Cyclo- N_5 . Dalton. Trans. **2018**, 47, 1398–1401.
- (12) Wang, P. C.; Xu, Y. G.; Wang, Q.; Shao, Y. L.; Lin, Q. H.; Lu, M. Self-Assembled Energetic Coordination Polymers Based on Multidentate Pentazole Cyclo- N_5^- . Sci. China Mater. **2018**, DOI: 10.1007/s40843-018-9268-0.
- (13) Zhang, W.; Wang, K.; Li, J.; Lin, Z.; Song, S.; Huang, S.; Zhang, Q. Stabilization of the Pentazolate Anion in a Zeolitic Architecture with Na₂₀N₆₀ and Na₂₄N₆₀ Nanocages. *Angew. Chem., Int. Ed.* **2018**, 57, 2592–2595.
- (14) Battaglia, S.; Evangelisti, S.; Leininger, T.; Faginas-L., o, N. Confinement of the Pentanitrogen Cation Inside Carbon N on tubes. In Computational Science and Its Applications ICCSA 2^18; Springer: Cham, 2018, 579–592.
- (15) Xu, Y.; Lin, Q.; Wang, P.; Lu, M. S. b. in of the Pentazolate Anion in Three Anhydrous and M. a. Free Energetic Salts. Chem. Asian J. 2018, 13, 924-928
- (16) Arhangelskis, M.; Katsenis, A. D.; Yor is, A. J.; Friščić, T. Computational Evaluation of Metal Penazolate Frameworks: Inorganic Analogues of Azolate Metal-Organic Frameworks. *Chem. Sci.* **2018**, *9*, 3367–3375.
- (17) Yu, T.; Ma, Y. D.; Lai, W. P.; Liu, Y. Z.; Ge, Z. X.; Ren. G. Roads to Pentazolate Anion: a Theoretical Insight. R. Soc. Of an Sc. 2018, 5, 172269.
- (18) Huang, R. Y.; Xu, H. Comment on "Sy.th sis and Characterization of the Pentazolate Anion Cy lo N_5 in $(N_5)_6(H_3O)_3(NH_4)_4Cl$. Science **2018**, 359, eaao3672
- (19) Jiang, C.; Zhang, L.; Sun, C.; Zhang, C.; Yang C., Chen, J.; Hu, B. Response to Comment on "Synthesis and Charac erization of the Pentazolate Anion Cyclo- N_5^- in $(N_5)_6(H,O)_7(NH_4)_4Cl$. Science 2018, 359, aas8953.
- (20) Marx, D.; Hutter, J. Ab Initio Mole uta. Dynamics: Basic Theory and Advanced Methods; Cambridge In ve.sity Press, 2009.
- (21) Hassanali, A. A.; Cuny, J. Verdolino, V.; Parrinello, M. Aqueous Solutions: State of the A. in Ab Initio Molecular Dynamics. *Philos. Trans. R. Soc., A* 201, 1, 272, 20120482.
- (22) Van Speybroeck V.; Hemelsoet, K.; Joos, L.; Waroquier, M.; Bell, R. G.; Catl. V., C. R. A. Advances in Theory and Their Application with the old of Zeolite Chemistry. *Chem. Soc. Rev.* 2015, 44, 70 4-11.
- (23) Bader, R. J. W. Atoms in Molecules. Acc. Chem. Res. 1985, 18, 9-15.
- (24) Lu, T.; Chen, F. Multiwfn: a Multifunctional Wavefunction Analyzer. J. Comput. Chem. 2012, 33, 580–592.
- (25) Grabowski, S. What is the Covalency of Hydrogen Bonding? Chem. Rev. 2011, 111, 2597–2625.

- (26) Steiner, T. The Hydrogen Bond in the Solid State. Angew. Chem., Int. Ed. 2002, 41, 48–76.
- (27) David, W. I.; Jones, M. O.; Gregory, D. H.; Jewell, C. M.; Johnson, S. R.; Walton, A.; Edwards, P. P. A Mechanism for Non-Stoichiometry in the Lithium Amide/Lithium Imide Hydrogen Storage Reaction. *J. Am. Chem. Soc.* **2007**, *129*, 1594–1601.
- (28) Mayo, S. L.; Olafson, B. D.; Goddard, W. A. DREIDING: a Generic Force Field for Molecular Simulations. *J. Phys. Chem.* **1990**, 94, 8897–8909.
- (29) Marenich, A. V.; Cramer, C. J.; Truhlar, D. G. Universal Solvation Model Based on Solute Electron Density and on a Continuum Model of the Solvent Defined by the Bulk Dielectric Constant and Atomic Surface Tensions. *J. Phys. Chem. B* **2009**, *113*, 6378–6396.
- (30) Zhang, J.; Zhang, H. Y.; Wu, T.; Wang, Q.; van der Spoel, D. Comparison of Implicit and Explicit Solvent Models for the Calculation of Solvation Free Energy in Organic Solvents. *J. Chem. Theory Comput.* **2017**, *13*, 1034–1043.
- (31) Hunter, E. P. L.; Lias, S. G. Evaluated Gas Phase Basicities and Proton Affinities of Molecules: an Update. *J. Phys. Chem. Ref. Data* 1998, 27, 413–656.
- (32) Hutter, J.; Iannuzzi, M.; Schiffmann, F.; VandeVondele, J. CP2K: Atomistic Simulations of Condensed Matter Systems. *J. Wires. Comput. Mol. Sci.* **2014**, *4*, 15–25.
- (33) Pera w, I. P.; Burke, K.; Ernzerhof, M. Generalized Gradient Approxi 1a. 5. Made Simple. Phys. Rev. Lett. 1997, 78, 1396-1396.
- (34) Chamber, S.; Antony, J.; Ehrlich, S.; Krieg, H. A Consistent and accurate Ab Initio Parametrization of Density Functional Dispersion Correction (DFT-D) for the 94 Elements H-Pu. J. Chem. Phys. 2010, 132, 154104.
- (35) Goedecker, S.; Teter, T.; Hutter, J. Separable Dual-space Gaussian Pseudopotentials. *Phys. Rev. B: Condens. Matter Mater. Phys.* 1996, 54, 1703–1710.
- (36) Lippert, G.; Hutter, J.; Parrinello, M. The Gaussian and Augmented-Plane-Very Density Functional Method for Ab Initio Molecular Dynamics Cimulations. *Theor. Chem. Acc.* **1999**, *103*, 124–140.
- (37) Lippe & G.; Hutter, J.; Parrinello, M. A Hybrid Gaussian and Plane Con Density Functional Scheme. *Mol. Phys.* **1997**, 92, 477–487
- (18) Bussi, G.; Donadio, D.; Parrinello, M. Canonical Sampling Through Velocity Rescaling. J. Chem. Phys. 2007, 126, 014101.
- (39) Henkelman, G.; Jónsson, H. A Dimer Method for Finding Saddle Points on High Dimensional Potential Surfaces using Only First Derivatives. *J. Chem. Phys.* **1999**, *111*, 7010–7022.
- (40) Ghysels, A.; Verstraelen, T.; Hemelsoet, K.; Waroquier, M.; Van Speybroeck, V. TAMkin: a Versatile Package for Vibrational Analysis and Chemical Kinetics. *J. Chem. Inf. Model.* **2010**, *50*, 1736–1750.
- (41) Zhao, Y.; Truhlar, D. G. The M06 Suite of Density Functionals for Main Group Thermochemistry, Thermochemical Kinetics, Noncovalent Interactions, Excited states, and Transition Elements: Two New Functionals and Systematic Testing of Four M06-class Functionals and 12 Other Functionals. *Theor. Chem. Acc.* 2008, 120, 215–241.
- (42) Dunning, T. H. Gaussian Basis Sets for Use in Correlated Molecular Calculations. I. The atoms boron through neon and hydrogen. *J. Chem. Phys.* **1989**, *90*, 1007–1023.
- (43) Woon, D. E.; Dunning, T. H. Gaussian Basis Sets for Use in Correlated Molecular Calculations. III. The atoms aluminum through argon. *J. Chem. Phys.* **1993**, *98*, 1358–1371.
- (44) Marenich, A. V.; Cramer, C. J.; Truhlar, D. G. Universal Solvation Model based on Solute Electron Density and on a Continuum Model of the Solvent Defined by the Bulk Dielectric Constant and Atomic Surface Tensions. *J. Phys. Chem. B* **2009**, *113*, 6378–6396.
- (45) Frisch, M. J.; Trucks, G. W.; Schlegel, H. B.; Scuseria, G. E.; Robb, M. A.; Cheeseman, J. R.; Scalmani, G.; Barone, V.; Mennucci,

B.; Petersson, G. A.; et al. *Gaussian 09*, revision B.01; Gaussian, Inc.: Wallingford CT, 2010.

(46) Kresse, G.; Furthmuller, J. Efficient Iterative Schemes for Ab Initio Total-Energy Calculations using a Plane-Wave Basis Set. *Phys. Rev. B: Condens. Matter Mater. Phys.* **1996**, 54, 11169–11186.

Solid Port Tools Solid Documents Comments Commen